Applied Physics B (2022) 128:64
https://doi.org/10.1007/s00340-022-07788-w

Applied Physics B
Lasers and Optics

REGULAR PAPER

Thermodynamic cost of quantum transfers

Sodeif Ahadpour[1] · **Forouzan Mirmasoudi**[1]

Received: 12 October 2021 / Accepted: 17 February 2022 / Published online: 8 March 2022

Abstract
We explain how thermodynamic cost can use for diagnosing optimal dense coding. We present a quantum channel where is included two initially uncorrelated thermal quantum systems to reveal the optimal dense coding using thermodynamic cost. The interest in dense coding brings into quantum correlation calculation. At first, the quantum Fisher information and spin squeezing are used to quantify the correlation dynamics over the system. The system reveals that the thermal evolution of quantum correlations depends crucially on specific energy and temperature. Also, they can be utilized as control parameters for optimal dense coding. Several interesting features of the variations of the energy cost and the dense coding capacity are obtained. It can keep its valid capacity value in a broad range of temperatures by increasing the energy value of excited states. Also, we can identify valid dense coding with the help of calculating the energy cost of the system. Using this approach, identifying a critical point of this model in dense coding capacity quality can be very effective.

1 Introduction

Studying the function of thermodynamics in information theory has provided a good insight into the quantum mechanics [1–4]. A focus on features of quantum correlations and entanglement conducted remarkably to the progress in our realization of the thermodynamics of quantum systems [2, 5, 6]. Up to now, the role and significance of thermodynamics in quantum information processing have fascinated the attention of many people [7, 8]. Moreover, the recognition of critical temperature in spin models is identified through different techniques [9].

The main objective of quantum mechanics is considered the quantum correlations, which not only contains a deeper understanding of the principles of quantum mechanics, but can also reveal an essential function of quantum information [10, 11] and enables the facility of quantum cryptographic protocol [12], quantum teleportation [13], quantum dense coding [14], and so forth. For example, in dense coding which is considered as an intriguing nonclassical implication, the sender can communicate two bits of classical information to the receiver by forwarding a single qubit if they mix a two-qubit maximally entangled state. Dense coding has been investigated not only theoretically [15–19] but also experimentally [20]. Along this line, much research has been devoted to study the quantum information and quantum correlation [21, 22] in various many-body systems [23].

To address the fundamental limitations inflicted by thermodynamics on the growth of correlations and entanglement in bipartite and multipartite settings, some systems have been inspected [24, 25]. In Ref. [25], the authors have studied the energy cost of the created correlations between the uncorrelated thermal quantum systems via performing such global unitary operations such as quantum discord and local quantum uncertainty. Therefore, anyone can ask whether other quantum correlations such as quantum Fisher information and spin squeezing can show a correlation in present thermodynamic limitations. Recently, it has been represented that quantum Fisher information provides a tool for understanding the phase sensitivity that systems can prepare for the imperfection of quantum measurement devices [26–28]. As a document of multipartite entanglement, it is asserted that it specifies topological states [29] and non-Gaussian many-body entangled states [30]. Quantum Fisher information can be widely explored in some intent such as the connection between quantum coherence and quantum phase transition [31–33], quantum metrology [34], and quantum speedup limit time [35]. Recently, it is attractive to find that spin squeezing is connected to quantum entanglement and one can use spin

✉ Sodeif Ahadpour
Ahadpour@uma.ac.ir

Forouzan Mirmasoudi
Fmirmasoudi@uma.ac.ir

[1] Physics Department, University of Mohaghegh Ardabili, P.O. Box 179, Ardabil, Iran

squeezing to characterize entanglement. It is found that spin squeezing relates to the minimum spin fluctuation in the plane perpendicular to the mean spin direction [36–38].

We know that correlated states play a significant role in dense coding. For this purpose, we present a straightforward calculation of how quantum Fisher information and also spin squeezing of states can occur the fundamental limitations coming from the initial temperature of two initially uncorrelated thermal quantum systems for building quantum correlations. The problem can be interested: how we can distinguish the connection between the dynamic properties of energy cost and dense coding capacity? Our results suggest that valid dense coding can be detected using the dynamic energy cost in thermodynamic effects.

The road map of this paper is formed as follows. In Sect. 2, we compute the density matrix for two initially uncorrelated two-dimensional thermal quantum systems, and then, we give out the analytical expression to the quantum Fisher information and spin squeezing and demonstrate how creating quantum correlations can be confined by the thermodynamics of the system. In Sect. 3, the super dense coding is discussed. We finish the paper with our main results and outlook in Sect. 4.

2 Creating quantum correlation between two thermal qubits

Let us take a global system can be included by two basic separable d-dimensional quantum systems A and B. And they link with a hot heat bath at temperature T, the Hamiltonian of each of which may be expressed as $H = \sum_{i=0}^{d-1} E_i|\psi_i\rangle\langle\psi_i|$, in which E_i and $|\psi_i\rangle$ are eigenvalues and eigenstates, respectively. The thermal state of this system at a temperature T is given by [7]

$$\rho_T = \rho \otimes \rho, \tag{1}$$

where $\rho = \frac{e^{-\beta H}}{\mathrm{Tr}(e^{-\beta H})}$, $\beta = 1/kT(k = 1)$, and k is the Boltzmann constant. In the following of discussion, we will stand for energy of the ground and excited state by $E_0 = 0$ and $E_1 = E$, respectively. Also, the initial thermal state of a qubit can be given as $\rho = p|0\rangle\langle 0| + (1-p)|1\rangle\langle 1|$. The coefficient p sets the ground populations that can be written

$$p = \frac{1}{1+e^{-\beta E}}. \tag{2}$$

As in Ref. [39] was showed the maximal entanglement of two-qubit arises by optimal global unitary operations. The global unitary operator U which is made in this protocol can be easily represented as two unitary operators ($U = V_2V_1$), so we can obtain the final state as$\rho_f = V_2V_1\rho_i V_1^\dagger V_2^\dagger$, where

$$V_1 = |00\rangle\langle 00| + |01\rangle\langle 01| + |11\rangle\langle 10| + |10\rangle\langle 11| \tag{3}$$

is the action of the *CNOT* gate and

$$V_2 = |\varphi_{00}\rangle\langle 00| + |01\rangle\langle 01| + |10\rangle\langle 10| + |\varphi_{11}\rangle\langle 11| \tag{4}$$

is a rotation in the subspace spanned by $|00\rangle, |11\rangle$ to maximally entangled states which are $|\varphi_{00}\rangle = \frac{1}{\sqrt{2}}(|00\rangle + |11\rangle)$ and $|\varphi_{11}\rangle = \frac{1}{\sqrt{2}}(|00\rangle - |11\rangle)$. Hence, the density matrix of the final state in the basis $|00\rangle, |10\rangle, |01\rangle, |11\rangle$ can be easily obtained by the following forms:

$$\rho_f = \begin{pmatrix} \frac{p}{2} & 0 & 0 & p^2 - \frac{p}{2} \\ 0 & p(1-p) & 0 & 0 \\ 0 & 0 & (1-p)^2 & 0 \\ p^2 - \frac{p}{2} & 0 & 0 & \frac{p}{2} \end{pmatrix}. \tag{5}$$

In the following, for obtaining quantum correlation, we focus on the quantum Fisher information and spin squeezing.

2.1 Fisher information between two thermal qubits

The quantum Fisher information (QF) is a widespread tool for explaining optimal validity in parameter estimation protocols [40–42]. An active area of research dedicated to evaluating the evolution of QF to determine the relation between quantum entanglement and quantum metrology [43, 44]. It has been illustrated that in the unitary evolution, quantum entanglement leads to a remarkable promotion in precision of parameter estimation. For an arbitrary parametric state ρ_θ that depends on θ, the QF is characterized as follows:

$$F^2(\rho_\theta) = \frac{1}{4}\mathrm{tr}(\rho_\theta L_\theta^2), \tag{6}$$

where L_θ is the symmetric logarithmic derivative operator. L_θ is defined as the solution of the equation

$$\frac{\partial \rho_\theta}{\partial \theta} = \frac{1}{2}(L_\theta\rho_\theta + \rho_\theta L_\theta). \tag{7}$$

The effect of the unitary evolution $U_\theta = e^{-iH\theta}$ on ρ, $\rho_\theta = U_\theta\rho U_\theta$, can be lead to parametric state ρ_θ. For a defined quantum state $\rho = \sum_l |\lambda_l\rangle\langle\lambda_l|$ with $\lambda_l \geqslant 0, \sum_l \lambda_l = 1$. Here, we stand for $F^2(\rho_\theta)$ with $F^2(\rho, H)$, which can also be expressed by [45]

$$F(\rho_f, H) = \frac{1}{2}\sum_{l\neq n} \frac{(\lambda_l - \lambda_n)^2}{\lambda_l + \lambda_n}|\langle l|H|n\rangle|^2. \tag{8}$$

According to Eq. (5), QFI can easily obtain as follows:

$$F(\rho_f, H) = \frac{(1-e^{-\beta E})^2}{2}\{\frac{1}{(1-e^{\beta E})^3} - \frac{1}{1+e^{2\beta E}}\}. \tag{9}$$

Obviously, if $T \to \infty$, $F(\rho_f, H)$ is equal to zero. Also, the maximal amount of the QF can be obtained in the limit $T \to 0$, which is equal to 0.5. In Fig. 1a, we plot the QF which has given in Eq. (9) to study the quantum correlations behavior with respect to initial temperature of the system. It is seen that the quantum correlations vanish completely

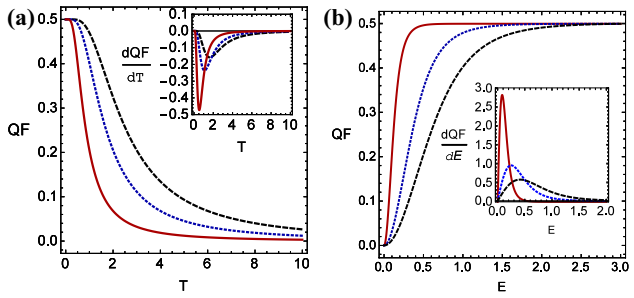

Fig. 1 **a** QF and the evolution of the first derivative of the QF versus T for various values of E ($E = 1$ (red , solid line), $E = 2$ (blue, dotted line), $E = 3$ (black, dashed line)). **b** QF and the evolution of the first derivative of the QF versus E for various values of T ($T = 0.1$ (red , solid line), $T = 0.3$ (blue, dotted line), $T = 0.5$ (black, dashed line))

after a threshold temperature for any specific energy. As can be observed for any specific energy E due to thermal fluctuations, QF is decreased by increasing temperature. Also, we see that by enhancing the energy value of excited states E, the threshold temperature is raised and, therefore, the QF can exist in a vast limit of temperature. It should be noted that the maximal value of the QF is equal to 0.5 which is obtained at $T = 0$. To further investigate the critical behavior of QF, we have plotted the first derivation of Fisher information with respect to initial temperature of the system for various values of E in Fig. 1a. It appears that the $\frac{dQF}{dT}$ have sharp dips in the thermal evolution for any specific energy E. A more detailed analysis shows that the position of the dips located at a critical temperature T_c. In fact, these sharp dips originate from the non-analytical property of QF at the critical temperature, which further demonstrates that the QF can detect the critical temperature for two initially uncorrelated thermal quantum systems. Now, we analyze the correspondence between the singularity of the threshold energy and the phase diagram for different temperatures. We have plotted QF and evolution of the first derivative QF with respect to the energy in Fig. 1b. From Fig. 1b, we see that with the increasing of energy for any special temperature, QF enhances to a maximum value. According to Fig. 1b, a threshold energy exists that depends on the temperature value. For a more detailed analysis, we display the evolution of the first derivative of the QF versus E in Fig. 1b. This graph reveals how the position of critical point energy alters as the temperature of the system increases.

2.2 Spin squeezing between two thermal qubits

Following Kitagawa and Ueda's [38] criterion of spin squeezing, we briefly review the definition of the spin squeezing parameter for a collection of N qubits with components $S^{\alpha} = \sum_{i=1}^{N} \frac{\sigma_i^{\alpha}}{2}, (\alpha \in x, y, z)$ as

$$\xi^2 = \frac{2(\Delta S_{\vec{n}_\perp})^2_{\min}}{J} = \frac{4(\Delta S_{\vec{n}_\perp})^2_{\min}}{N}. \tag{10}$$

Here, the subscript $\vec{n}_\perp$ refers to an axis perpendicular to angular momentum operator. $S = (S_x, S_y, S_z)$ denotes the angular momentum operator of an ensemble of spin-1/2 particles. Where $(\Delta S_{\vec{n}_\perp})^2_{\min}$ is the minimal spin fluctuation in a plane perpendicular to the mean spin, and $J = \frac{N}{2}$, and $S_{\vec{n}_\perp} = \vec{S}.\vec{n}_\perp$. The non-correlated limit yields $\xi^2 = 1$, while the inequality $\xi^2 < 1$ indicates that the system is spin squeezed and entangled. In Ref [46] was indicated for the mean spin along the z direction spin squeezing can be written as

$$\xi^2 = 1 + \frac{N}{2} - \frac{2}{N}[\langle S_z^2\rangle + |\langle S_+^2\rangle|], \tag{11}$$

where $S_{\pm} = S_x \pm S_y$ are the ladder operators. From Eq. (11), we see that the squeezing parameter is determined by a sum of two expectation values $\langle S_z^2\rangle$ and $\langle S_+^2\rangle$; hence, the calculations are greatly simplified. For this density matrix Eq.(5), the associated spin squeezing is given by

$$\xi^2 = 1 - \frac{1}{4}\tanh\frac{\beta E}{2}\left(1 + \tanh\frac{\beta E}{2}\right). \tag{12}$$

According to Eq. (12), it is clear that the maximal value of the spin squeezing is equal to 1, which is obtained at $T \to \infty$. Also, the minimal amount of the infinity can be obtained in the limit $T \to 0$. Variations of spin squeezing are given in Fig. 2a for any specific energy E. We can see the spin squeezing undergoes to value one with increasing temperature of the system for any specific energy. As a physical interpretation, the interaction between the system with its environment at high temperatures can be lead to non-squeezed states. Notably, previous studies [25] have shown that the entanglement vanished completely at a finite critical temperature. It is also known in which all the specific energy

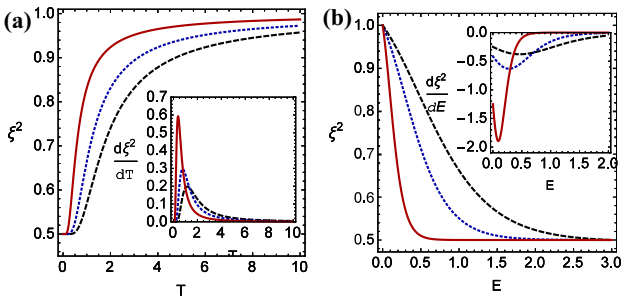

Fig. 2 **a** Spin squeezing and the evolution of the first derivative of the spin squeezing versus T for various values of E ($E = 1$ (red , solid line), $E = 2$ (blue, dotted line), $E = 3$ (black, dashed line)) **b** spin squeezing and the evolution of the first derivative of the spin squeezing versus E for various values of T ($T = 0.1$ (red , solid line), $T = 0.3$ (blue, dotted line), $T = 0.5$ (black, dashed line))

is supplied at a low temperature has a spin squeezing efficient. Therefore, low temperature can maintain squeezing. Having this in mind, the first derivative of the spin squeezing is depicted as a function of T in Fig. 2a. The derivative of spin squeezing versus temperature of the system shows a singular behavior at the critical temperature for any specific energy E. As, the spin squeezing constructs a maximum at the critical temperature. In generally, It can be seen how the temperature of the initial state affects the amount of correlation that we can be created. To confirm the previous discussions, we investigate the behavior of the spin squeezing and the first derivative of the spin squeezing versus energy E for the difference of temperatures in Fig. 2b. We find that spin squeezing exhibits a sudden change at the critical point. This indicates that spin squeezing can be used to detect the phase transition that has happened in initially uncorrelated thermal quantum systems.

3 Superdense coding

Now, we carry out the thermal optimal dense coding in a global system consisting of two initially uncorrelated d-dimensional quantum systems A and B as a quantum channel. For this purpose, the set of mutually orthogonal unitary transformations is necessary to be made. The set of mutually orthogonal unitary transformations for two-qubit are given as follows [47]:

$$\begin{aligned} U_{00}|j\rangle &= |j\rangle \\ U_{01}|j\rangle &= |j+1(mod2)\rangle \\ U_{10}|j\rangle &= e^{\sqrt{-1}(2\pi/2)j}|j\rangle \\ U_{11}|j\rangle &= e^{\sqrt{-1}(2\pi/2)j}|j+1(mod2)\rangle, \end{aligned} \tag{13}$$

where $|j\rangle$ is the single qubit computational basis ($|j\rangle = |0\rangle, |1\rangle$). The average state of the ensemble of signal states generated by the unitary transformations Eq. (13) is given by

$$\overline{\rho^*} = \frac{1}{4}\sum_{i=0}^{3}(U_i \otimes I_2)\rho(U_i^\dagger \otimes I_2), \tag{14}$$

where 0 stands for 00, 1 for 01, 2 for 10, 3 for 11, and ρ is the density matrix of the quantum channel. Equation (13) represents the operations that Alice (sender) performs on the shared entangled state ρ. If the sender does the set of mutually orthogonal unitary transformations, the maximum dense coding capacity χ can be obtained by

$$\chi = S(\overline{\rho^*}) - S(\rho), \tag{15}$$

where $S(\overline{\rho^*})$ is a von Neumann entropy for the average state of an ensemble of signal states $\overline{\rho^*}$, and $S(\rho)$ is the von Neumann entropy of the quantum channel. If $\chi > 1$ dense coding is valid, and for optimal dense coding χ must be the maximum, i.e., $\chi_{\max} = 2$. We are now ready to discuss the validity of the generated quantum correlation a global system consisted of two initially uncorrelated d-dimensional quantum systems A and B in contact with a heat bath at temperature T as a quantum channel to study the optimal dense coding. By considering the density matrix Eq. (5), we first focus on the thermal dense coding capacity. By numerical calculation, we can plot dense coding capacity as a function T for different specific energy values. In Fig. 3a, we observe valid dense coding for any specific energy in low temperatures. It is reduced from the maximum to zero in a short interval of temperature and disappears for the large amounts of T. The increase in the energy value of excited states helps dense coding capacity can be alive in a broad range of temperature.

Now, we start to explore a work cost W to the optimal dense coding. Thermodynamic cost of dense coding W is given by [7, 48, 49]

$$W = \mathrm{Tr}\,(H_{tot}\rho^*) - \mathrm{Tr}\,(H_{tot}\rho_f), \tag{16}$$

where ρ^* is the final state Eq. (14) as follows:

$$\rho^* = \begin{pmatrix} \frac{p^2-\frac{3p}{2}+1}{2} & 0 & 0 & 0 \\ 0 & \frac{p(3-2p)}{4} & 0 & 0 \\ 0 & 0 & \frac{p(3-2p)}{4} & 0 \\ 0 & 0 & 0 & \frac{p^2-\frac{3p}{2}+1}{2} \end{pmatrix}, \tag{17}$$

and $H_{tot} = \sum_i H^{(i)}$ is the total Hamiltonian as

$$H_{tot} = H \otimes I_2 + I_2 \otimes H = \begin{pmatrix} 0 & 0 & 0 & 0 \\ 0 & E & 0 & 0 \\ 0 & 0 & E & 0 \\ 0 & 0 & 0 & 2E \end{pmatrix}. \tag{18}$$

By substituting Eqs. (5), (18) and (17) into Eq. (16), work cost can be obtained as

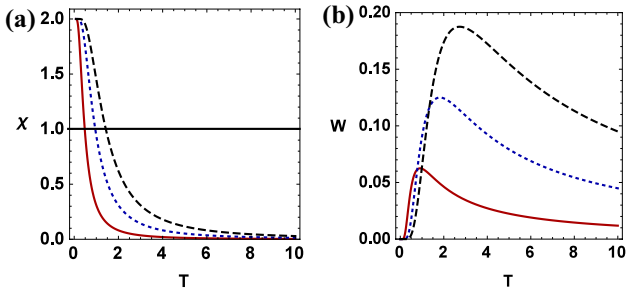

Fig. 3 **a** Dense coding capacity and **b** energy cost of dense coding versus T for various values of E ($E = 1$ (red , solid line), $E = 2$ (blue, dotted line), and $E = 3$ (black, dashed line))

$$W = \frac{e^{\beta E} - 1}{2(e^{\beta E} + 1)^2} E. \tag{19}$$

We find that the energy cost is dependent on temperature and specific energy. According to Eq. (19), it is easy to prove that value of the energy cost can be maximal in the critical temperature $T_c = 0.91E$ which the dense coding is not valid, i.e., $\chi < 1$ (see Fig. 3a). In Fig. 3b, the energy cost of dense coding is plotted as a function of temperature for any specific energy. It can be seen when the temperature is smaller than T_c, the energy cost increases until its maximum value with raising the temperature. However, it for $T > T_c$ specific energy exhibits a collapse as temperature increases. Moreover, the range of T for energy cost is also broadened as specific energy increases in this interval. Notably, the height of peaks energy cost changes manifestly. It approaches the higher peak by increasing specific energy. Comparing dynamic energy cost Fig. 3b and dense coding capacity Fig. 3a leads to an interesting outcome, there is no optimal dense coding when energy cost is decreasing, i.e., after the phase transition $T > T_c$. We notice that when $T < T_c$, until the energy cost reaches its maximum value, we can obtain optimal dense coding. With these results at hand, one can detect optimal dense coding via the behavior of energy cost. Therefore, it is helpful to investigate the energy cost as indicators of valid dense coding in every system.

4 Conclusion

In conclusion, we have prospected the number of quantum correlations that can be made between two initially uncorrelated thermal quantum systems via an optimal protocol that maximizes the quantum correlation. We inspected the thermal evolution of quantum correlations such as quantum Fisher information and spin squeezing in this system. It is illustrated that increasing the initial equilibrium temperature leads to diminishing the amount of quantum correlations that can be caused between two thermal states. Quantum correlations undergo an abrupt death at the critical temperature. Moreover, we have investigated the quantum dense coding for this model. We have found appealing results as the existence of a relationship between dense coding and energy cost that will certainly lead to a better comprehension of the non-equilibrium systems. Our analyses have indicated by enhancing the value of temperature, the value of energy cost tends to its maximum. Interestingly, after crossing the critical temperature, when no optimal dense coding exists in the system, the energy cost of dense coding becomes spoiled. We offer these features as a tool to detect optimal dense coding.

Author Contributions FM developed the theoretical formalism, performed the analytic calculations, and performed the numerical simulations. Both FM and SA authors contributed to the final version of the manuscript. SA supervised the project.

References

1. K. Maruyama, F. Nori, V. Vedral, Colloquium: the physics of Maxwell's demon and information. Rev. Mod. Phys. **81**(1), 1 (2009)
2. M. Horodecki, J. Oppenheim, Fundamental limitations for quantum and nanoscale thermodynamics. Nat. Commun. **4**(1), 1–6 (2013)
3. S. Ahadpour, F. Mirmasoudi, Coupled two-qubit engine and refrigerator in Heisenberg model. Quantum Inf. Process. **20**(2), 1–13 (2021)
4. S. Haddadi, A. Akhound, Thermal entanglement properties in two qubits one-axis spin squeezing model with an external magnetic field. Int. J. Theor. Phys. **58**(2), 399–402 (2019)
5. L. Del Rio, J. Åberg, R. Renner, O. Dahlsten, V. Vedral, The thermodynamic meaning of negative entropy. Nature **474**(7349), 61–63 (2011)
6. M. Horodecki, J. Oppenheim, (Quantumness in the context of) resource theories. Int. J. Mod. Phys. B **27**, 1345019 (2013)
7. M. Huber, M. Perarnau-Llobet, K.V. Hovhannisyan, P. Skrzypczyk, C. Klöckl, N. Brunner, A. Acín, Thermodynamic cost of creating correlations. New J. Phys. **17**(6), 065008 (2015)
8. S. Ahadpour, F. Mirmasoudi, Thermal quantum discord and super quantum discord teleportation via a two-qubit spin-squeezing model. Theor. Math. Phys. **195**(1), 625–639 (2018)
9. C. Alexandrou, A. Athenodorou, C. Chrysostomou, S. Paul, The critical temperature of the 2d-Ising model through deep learning autoencoders. Eur. Phys. J. B **93**(12), 1–15 (2020)
10. M.A. Nielsen, I. Chuang, *Quantum Computation and Quantum Information* (Cambridge University Press, Cambridge, 2002)
11. S. Ahadpour, F. Mirmasoudi, Dynamics of quantum correlations for different types of noisy channels. Opt. Quant. Electron. **52**(8), 1–14 (2020)
12. A.K. Ekert, Quantum cryptography based on Bell's theorem. Phys. Rev. Lett. **67**(6), 661 (1991)
13. C.H. Bennett, G. Brassard, C. Crépeau, R. Jozsa, A. Peres, W.K. Wootters, Teleporting an unknown quantum state via dual classical and Einstein-Godolsky-Rosen channels. Phys. Rev. Lett. **70**(13), 1895 (1993)
14. C.H. Bennett, S.J. Wiesner, Communication via one-and two-particle operators on Einstein-Podolsky-Rosen states. Phys. Rev. Lett. **69**(20), 2881 (1992)
15. A. Barenco, A.K. Ekert, Dense coding based on quantum entanglement. J. Mod. Opt. **42**(6), 1253–1259 (1995)
16. S.L. Braunstein, H.J. Kimble, in *Quantum Information with Continuous Variables*. (Springer, New York, 2000), pp. 95–103
17. S. Bose, M.B. Plenio, V. Vedral, Mixed state dense coding and its relation to entanglement measures. J. Mod. Opt. **47**(2–3), 291–310 (2000)
18. F. Mirmasoudi, S. Ahadpour, Dynamics of super quantum discord and optimal dense coding in quantum channels. J. Phys. A Math. Theor. **51**(34), 345302 (2018)
19. F. Mirmasoudi, S. Ahadpour, Application quantum renormalization group to optimal dense coding in transverse Ising model. Physica A **515**, 232–239 (2019)
20. K. Mattle, H. Weinfurter, P.G. Kwiat, A. Zeilinger, Dense coding in experimental quantum communication. Phys. Rev. Lett. **76**(25), 4656 (1996)

21. S. Haddadi, M. Bohloul, A brief overview of bipartite and multipartite entanglement measures. Int. J. Theor. Phys. **57**(12), 3912–3916 (2018)
22. S. Szalay, Multipartite entanglement measures. Phys. Rev. A **92**(4), 042329 (2015)
23. M.-L. Hu, X. Hu, J. Wang, Y. Peng, Y.-R. Zhang, H. Fan, Quantum coherence and geometric quantum discord. Phys. Rep. **762**, 1–100 (2018)
24. A. Misra, U. Singh, S. Bhattacharya, A.K. Pati, Energy cost of creating quantum coherence. Phys. Rev. A **93**(5), 052335 (2016)
25. N. Behzadi, E. Soltani, E. Faizi, Thermodynamic cost of creating global quantum discord and local quantum uncertainty. Int. J. Theor. Phys. **57**(10), 3207–3214 (2018)
26. M.G. Paris, Quantum estimation for quantum technology. Int. J. Quantum Inf. **7**(supp01), 125–137 (2009)
27. S.L. Braunstein, C.M. Caves, G.J. Milburn, Generalized uncertainty relations: theory, examples, and Lorentz invariance. Ann. Phys. **247**(1), 135–173 (1996)
28. H. Cheraghi, S. Mahdavifar, Dynamics of coherence: Maximal quantum fisher information versus Loschmidt echo. Phys. Rev. B **102**(2), 024304 (2020)
29. Y.-R. Zhang, Y. Zeng, H. Fan, J. You, F. Nori, Characterization of topological states via dual multipartite entanglement. Phys. Rev. Lett. **120**(25), 250501 (2018)
30. H. Strobel, W. Muessel, D. Linnemann, T. Zibold, D.B. Hume, L. Pezzè, A. Smerzi, M.K. Oberthaler, Fisher information and entanglement of non-gaussian spin states. Science **345**(6195), 424–427 (2014)
31. T.-L. Wang, L.-N. Wu, W. Yang, G.-R. Jin, N. Lambert, F. Nori, Quantum fisher information as a signature of the superradiant quantum phase transition. New J. Phys. **16**(6), 063039 (2014)
32. P. Zanardi, M.G. Paris, L.C. Venuti, Quantum criticality as a resource for quantum estimation. Phys. Rev. A **78**(4), 042105 (2008)
33. B. Raffah, S. Abdel-Khalek, K. Berrada, E. Khalil, Y. Al-Hadeethi, N. Almalky, M. Wahiddin, Quantum correlations and quantum fisher information of two qubits in the presence of the time-dependent coupling effect. Eur. Phys. J. Plus **135**(6), 1–10 (2020)
34. B. Escher, R. de MatosFilho, L. Davidovich, General framework for estimating the ultimate precision limit in noisy quantum-enhanced metrology. Nat. Phys. **7**(5), 406–411 (2011)
35. M.M. Taddei, B.M. Escher, L. Davidovich, R.L. de Matos Filho, Quantum speed limit for physical processes. Phys. Rev. Lett. **110**(5), 050402 (2013)
36. A.S. Sørensen, K. Mølmer, Entanglement and extreme spin squeezing. Phys. Rev. Lett. **86**, 4431–4434 (2001)
37. D.J. Wineland, J.J. Bollinger, W.M. Itano, D.J. Heinzen, Squeezed atomic states and projection noise in spectroscopy. Phys. Rev. A **50**, 67–88 (1994)
38. M. Kitagawa, M. Ueda, Squeezed spin states. Phys. Rev. A **47**(6), 5138 (1993)
39. F. Verstraete, K. Audenaert, B. De Moor, Maximally entangled mixed states of two qubits. Phys. Rev. A **64**(1), 012316 (2001)
40. C.W. Helstrom, *Quantum Detection and Estimation Theory*, vol. 3 (Academic Press, New York, 1976)
41. S.M. Kay, *Fundamentals of Statistical Signal Processing* (Prentice Hall PTR, New Jersey, 1993)
42. M.G. Genoni, S. Olivares, M.G. Paris, Optical phase estimation in the presence of phase diffusion. Phys. Rev. Lett. **106**(15), 153603 (2011)
43. F. Chapeau-Blondeau, Entanglement-assisted quantum parameter estimation from a noisy qubit pair: A fisher information analysis. Phys. Lett. A **381**(16), 1369–1378 (2017)
44. V. Giovannetti, S. Lloyd, L. Maccone, Quantum-enhanced measurements: beating the standard quantum limit. Science **306**(5700), 1330–1336 (2004)
45. M.N. Bera, Role of Quantum Correlation in Metrology Beyond Standard Quantum Limit, arXiv preprint. arXiv:1405.5357 (2014)
46. X. Wang, B.C. Sanders, Spin squeezing and pairwise entanglement for symmetric multiqubit states. Phys. Rev. A **68**(4), 012101 (2003)
47. T. Hiroshima, Optimal dense coding with mixed state entanglement. J. Phys. A Math. Gen. **34**(35), 6907 (2001)
48. G. Watanabe, B.P. Venkatesh, P. Talkner, A. Del Campo, Quantum performance of thermal machines over many cycles. Phys. Rev. Lett. **118**(5), 050601 (2017)
49. A. Hewgill, A. Ferraro, G. De Chiara, Quantum correlations and thermodynamic performances of two-qubit engines with local and common baths. Phys. Rev. A **98**(4), 042102 (2018)